



Why do general circulation models overestimate the aerosol cloud lifetime effect? A case study comparing CAM5 and a CRM

Cheng Zhou and Joyce E. Penner

Department of Climate and Space Sciences and Engineering, University of Michigan, Ann Arbor, Michigan, USA

Correspondence to: Cheng Zhou (zhouc@umich.edu)

Received: 11 July 2016 – Published in Atmos. Chem. Phys. Discuss.: 21 July 2016

Revised: 7 December 2016 – Accepted: 8 December 2016 – Published: 2 January 2017

Abstract. Observation-based studies have shown that the aerosol cloud lifetime effect or the increase of cloud liquid water path (LWP) with increased aerosol loading may have been overestimated in climate models. Here, we simulate shallow warm clouds on 27 May 2011 at the southern Great Plains (SGP) measurement site established by the Department of Energy's (DOE) Atmospheric Radiation Measurement (ARM) program using a single-column version of a global climate model (Community Atmosphere Model or CAM) and a cloud resolving model (CRM). The LWP simulated by CAM increases substantially with aerosol loading while that in the CRM does not. The increase of LWP in CAM is caused by a large decrease of the autoconversion rate when cloud droplet number increases. In the CRM, the autoconversion rate is also reduced, but this is offset or even outweighed by the increased evaporation of cloud droplets near the cloud top, resulting in an overall decrease in LWP. Our results suggest that climate models need to include the dependence of cloud top growth and the evaporation/condensation process on cloud droplet number concentrations.

with increasing aerosol particles depending on factors like mesoscale cloud cellular structures, dryness of the free troposphere, and boundary layer depth (Christensen and Stephens, 2011; Chen et al., 2012, 2015). Results from large-eddy simulations (LESs) and cloud resolving models (CRM) show the response of cloud water to aerosols is complicated by competing effects like reduced precipitation formation efficiency in clouds and enhanced evaporation at the cloud top or in the downdraft regions of cloud edges (Ackerman et al., 2004; Xue and Feingold, 2006; Tao et al., 2012). Since CRMs and LES models resolve clouds, have more complete physics, and depend less on subgrid parameterizations than general circulations models (GCMs), they are often used together with field measurements to evaluate and improve parameterizations of clouds and radiation used in climate models. Several previous studies have compared single-column models, which are essentially an isolated column of a GCM and cloud resolving models (Moncreiff et al., 1997; Ghan et al., 2000; Xu et al., 2002; Xie et al., 2002, 2005). Lee and Penner (2010) extended these types of comparisons to the response of the two models (CAM and a CRM) to increases in aerosols in thin non-precipitating marine stratocumulus. Both models found that LWP increased but the effect from increased condensation dominated in the CRM while the effect from decreased autoconversion dominated in CAM. Wang et al. (2012) used satellite observations of the precipitation frequency susceptibility together with model simulations to constrain cloud lifetime effects in warm marine clouds simulated in GCMs. They show that GCMs tend to overestimate the precipitation frequency susceptibility of marine clouds. Since the LWP increase as a result of increased cloud condensation nuclei concentrations is highly correlated with precipitation frequency susceptibility in climate models, they

1 Introduction

Traditionally aerosols have been thought to lengthen cloud lifetime (Albrecht, 1989) by increasing droplet number and reducing droplet size thereby delaying and reducing the formation of rain in clouds. These longer-lived clouds would then increase cloud cover and reflect more sunlight. Yet observational evidence for these lifetime effects is limited and contradictory (Boucher et al., 2013). Observations of ship tracks show that the liquid water path (LWP) in marine boundary-layer clouds can either increase or decrease

surmise that the LWP increase is too high and show that this overestimation could be “fixed” by reducing the dependence of the autoconversion rate on cloud droplet number in the models.

In this study, we simulated continental shallow warm clouds with a very small precipitation rate ($<0.1 \text{ mm day}^{-1}$) observed on 27 May 2011 at the southern Great Plains (SGP) measurement site established by the Department of Energy’s (DOE) Atmospheric Radiation Measurement (ARM) program using the single-column version of a global climate model (CAM, version 5.3) and a cloud resolving model and explored plausible causes for the differences in the response of these two models to increases in aerosols. Here, we specifically identify that the cloud top growth and turbulence mixing parameterizations within CAM require improvement, rather than only the autoconversion rate. Section 2 describes the models and setup. Section 3 presents results followed by conclusions and a discussion in Sect. 4.

2 Description of models and setup

We used the Goddard Cumulus Ensemble (GCE) model with recent improvements (Tao et al., 2014) and the single-column version of Community Atmosphere Model (CAM, version 5.3) which is the atmospheric component of the Community Earth System Model (CESM, version 1.2.2). Readers are referred to Neale et al. (2012) for more model details of CAM. Here, we briefly summarize the two most critical parameterizations for warm stratus clouds in CAM: cloud microphysics and cloud macrophysics. The cloud microphysics is a two-moment scheme (Morrison et al., 2005; Morrison and Gettelman, 2008 – MG, version 1.5) which predicts the number concentrations and mixing ratios of cloud droplets. The source term for the cloud droplets in warm clouds only includes the activation of cloud condensation nuclei while the sink terms include the instantaneous evaporation of falling cloud droplets into the clear portions of grids beneath clouds, autoconversion of cloud droplets to form rain, and accretion of cloud droplets by rain. The first two sink terms (instantaneous evaporation of falling cloud droplets and autoconversion) depend on the aerosol number concentration since the terminal falling speed of cloud droplets is related to cloud droplet size and the autoconversion rate is inversely proportional to cloud droplet number ($\sim N_c^{-1.79}$ where N_c is the in-cloud cloud droplet number). The last sink term (accretion) does not depend on the cloud droplet number (Khairoutdinov and Kogan, 2000). In-cloud cloud water variability within a GCM grid is based on observed cloud optical depth variability in marine boundary layer clouds. Thus, the sub-grid in-cloud water mixing (q_c'') follows a gamma distribution $P(q_c'') = \frac{q_c''^{\nu-1} \alpha^\nu}{\Gamma(\nu)} \exp(-\alpha q_c'')$, where $\alpha = 1/q_c'$, q_c' is mean in-cloud mixing ratio and ν is chosen to be 1 for simplicity. This sub-grid variability func-

tion is used to derive factors which can then be applied to calculate microphysical process rates using only the mean in-cloud mixing ratios. The conversion of water vapor to cloud condensate is computed by the cloud macrophysics parameterization which also predicts the cloud fraction in each grid as well as the horizontal and vertical overlapping structures of clouds. Following Smith (1990), the liquid fraction of stratus clouds in CAM5 is derived from an assumed triangular distribution of total relative humidity (i.e., the sum of water vapor and liquid cloud water). The net conversion rate of water vapor to stratus condensate is diagnosed using saturation equilibrium conditions as follows: (1) the RH over the water within the liquid stratus is always 100 %, and (2) no liquid stratus droplets exist in the clear portion of the grid.

The GCE model is a CRM that has been developed and improved at the NASA Goddard Space Flight Center. Its development and main features were published in Tao and Simpson (1993) and Tao et al. (2003) and recent improvements and applications were presented in Tao et al. (2014). The GCE model used in the present paper uses the double moment version of the Colorado State University Regional Atmospheric Modeling System (RAMS) bulk microphysics scheme (Saleeby and Cotton, 2004) which assumes a gamma-shaped particle size distribution for three species of liquid (small and large cloud droplets and rain). The small cloud droplets range from 2 to 40 microns in diameter, and the large cloud droplets range from 40 to 80 microns. Collection of cloud droplets is simulated using stochastic collection equation solutions, facilitated by bin-emulating lookup tables. A positive definite advection scheme is used for scalar variables (Smolarkiewicz and Grabowski, 1990). Sub-grid-scale (turbulent) processes are parameterized using a scheme based on Klemp and Wilhelmson (1978) and Soong and Ogura (1980). The effects of both dry and moist processes on the generation of sub-grid-scale kinetic energy have been incorporated. Readers are referred to Lee et al. (2009) and Tao et al. (2014) for more detailed descriptions of the model physics.

CAM has 30 vertical layers and a variable vertical resolution which depends on the surface pressure and the vertical temperature profile. In the case studied in this paper the vertical resolution is roughly 100 m near the surface and stretches to about 300 m at 2 km decreasing to ~ 1 at 10 km. The time step is 20 min. GCE has 128 grids in the two horizontal directions and 144 vertical layers. The horizontal resolution is 50 m, so the domain size is 6.4 km \times 6.4 km. GCE also uses a stretched vertical resolution that varies from about 30 m near the surface to about 90 m at 2 km and further to ~ 200 m at 10 km. The time step of the GCE model is 1 s. Both models use the same initial conditions (surface pressure and temperature, and vertical temperature, water vapor and wind profiles) and boundary conditions (surface sensible and latent heat fluxes as well as surface pressure and temperature). Advective tendencies of temperature and moisture (both vertically and horizontally) are specified based on an

objective variational analysis approach (Xie et al., 2014) fit to the Midlatitude Continental Convective Clouds Experiment (MC3E) campaign observations which were conducted from April to June 2011 near the DOE ARM SGP site. The analyzed advective tendencies cover the period from 22 April to 21 June 2011. Middle to deep convective clouds were observed on most cloudy days. For this study, 27 May 2011 was selected because middle and high clouds were absent during a low cloud period observed near noon. The vertical wind, temperature, moisture and cloud fraction profiles, surface latent and sensible heat fluxes as well as the advective tendencies of temperature and moisture are shown in Fig. S1 in the Supplement. Low clouds occurred from ~ 1 to ~ 2 km near the top of the boundary layer and were strongly modulated by the advective tendencies of temperature and moisture. Positive moisture flux and negative temperature flux were observed during the growing stage of the clouds while negative moisture flux and positive temperature flux were observed during the decaying stage. Both models are initialized at 00:00 LT (local time) and run for 18 h.

To study the effect of aerosols on clouds, we scaled the aerosol vertical profiles in both models by increasing the surface aerosol number concentrations from 250 to 4000 cm^{-3} . GCE uses a prescribed aerosol profile which decreases linearly from its surface concentration to 100 cm^{-3} at an altitude of 14 km and above. The activation of aerosols to cloud droplets is based on the grid resolved vertical updraft velocity, temperature, and aerosol number and size from a lookup table constructed from results of a Lagrangian parcel model (Saleeby and Cotton, 2004). For CAM, we extracted the averaged aerosol profile in May at this location from a 5-year run of CAM5 using the MAM3 aerosol module and scaled the aerosol profile based on the surface aerosol number concentrations (see Fig. S2 for profiles of aerosol number concentrations used in the two models). The activation of aerosols into cloud droplets in CAM is diagnosed as a function of the modeled subgrid-scale updraft velocity and aerosol compositions/sizes/numbers (Abdul-Razzak and Ghan, 2000). Even though we set the total surface aerosol number concentrations the same in the two models, the aerosol composition, size and number at cloud level, and the nucleation schemes are inherently different. However, since this paper focuses on a sensitivity study which is aimed at revealing the different cloud physical representations in the two models that lead to *opposite* responses of the simulated LWP to increasing aerosol number concentrations that cover a wide range (250 to 4000 cm^{-3}) rather than quantifying the changes of the LWP, these differences are not critical to the conclusions of the paper. To better isolate differences in the aerosol indirect effect in the two models, we also turned off the aerosol direct radiative effect.

3 Results

Figure 1a shows the observed cloud fractions from the early morning to the late afternoon on 27 May 2011 at the SGP site, while Fig. 1b and c show the simulated mean cloud water content from the two models assuming a surface aerosol number concentration of 500 cm^{-3} . Compared to the observations, the simulated clouds from both models begin later in the day and have a smaller vertical coverage. But the models compare relatively well to each other which suggests that differences between the models and the observations may largely be caused by the possible errors/uncertainties associated with the derived initial conditions or advective tendencies. Nevertheless, we can see that the GCE model captures the observed growth of the clouds with height while CAM does not. A detailed analysis of the GCE (next paragraph) shows that the clouds could be loosely classified as stratocumulus which occur near the top of the planetary boundary layer (PBL) and are mainly driven by long-wave radiative cooling offset by short-wave radiative heating. This is corroborated by CAM's result which shows all simulated clouds are stratus clouds and no convective clouds are able to form above the PBL. The advective tendencies of heat and moisture also strongly modulate the clouds. For example, the positive moisture tendency before 14:00 leads to slightly larger in-cloud water vapor mixing ratio than that below the clouds (more details will be presented in the discussion of Fig. 2).

Figure 1d and e show the domain-averaged liquid water path (LWP) from the two models for five different surface aerosol number concentrations (250, 500, 1000, 2000, and 4000 cm^{-3}). Both models underestimate the LWP during the day, similar to their underestimation of cloud cover. GCE shows relatively small changes in the LWP when using different surface aerosol numbers. The LWP slightly increases with the increasing aerosol number before $\sim 14:00$ but starts to decrease with the increasing aerosol number when the clouds start to decay after around 14:00. On the other hand, the LWP from CAM increases substantially and consistently with increasing aerosol number and matches the observed LWP better when the surface aerosol number is equal to 4000 cm^{-3} . As noted earlier, due to uncertainties associated with the derived forcing data as well as uncertainties in the models, this should not be interpreted as proof that CAM represents the physics better.

Figure 1f and g show the precipitation rates from the two models. The precipitation rate from CAM consistently decreases with increasing aerosol number and is nearly suppressed after 13:00. The change is most prominent when the aerosol number is increased from 250 to 500 cm^{-3} . This result is due to a combination of decreased autoconversion/accretion and increased evaporation of rain. When the aerosol number is increased from 250 to 500 cm^{-3} , the sum of autoconversion/accretion decreases. Meanwhile, since there is less rain falling through the unsaturated sub-cloud layers, the final fraction of rain which can survive

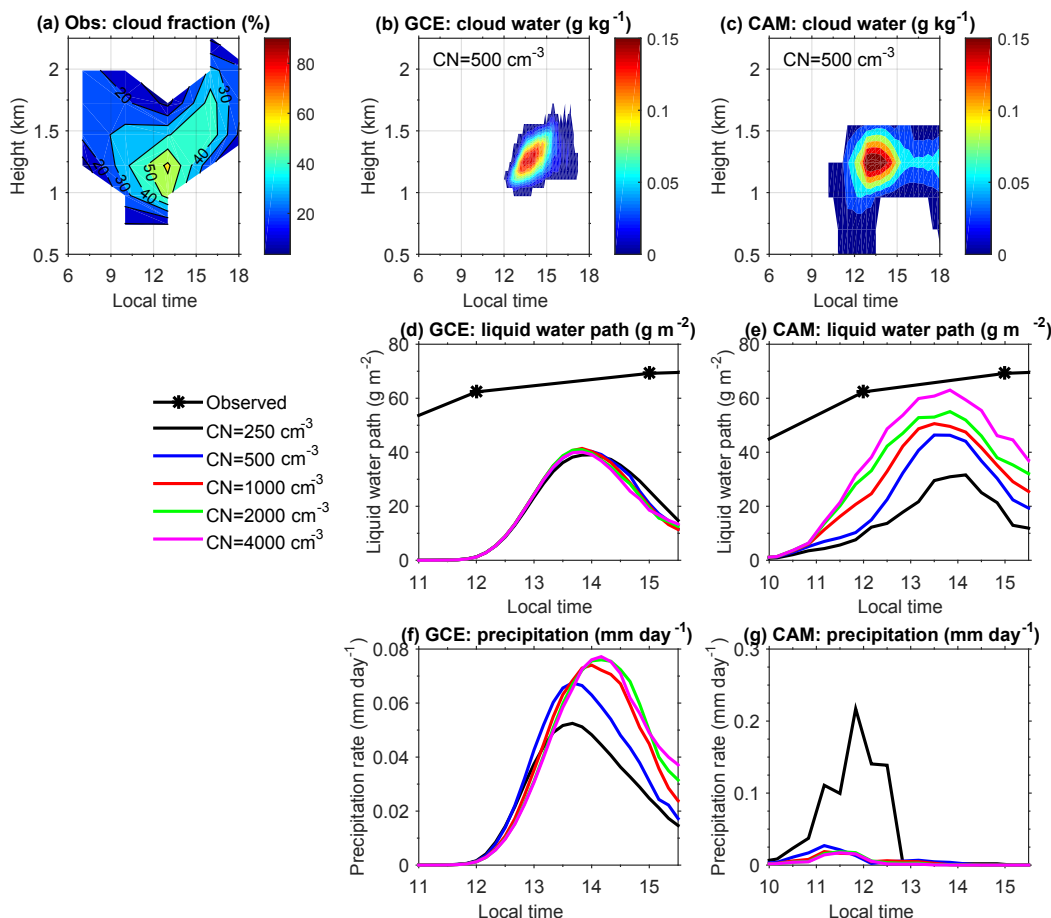


Figure 1. (a) Observed cloud fractions on 27 May 2011 at the SGP site. Domain-averaged cloud water content from the GCE model (b) and the single-column version of CAM (c) for the case assuming a surface aerosol number of 500 cm^{-3} . Liquid water path and surface precipitation rates from GCE (d, f) and CAM (e, g) with varying surface aerosol number concentrations.

evaporation also decreases. The relatively large decrease of surface precipitation is peculiar to the aerosol numbers and environmental conditions simulated here. The precipitation rates from GCE are overall very small with maximum values less than 0.08 mm day^{-1} . The change in precipitation for GCE with increasing aerosol numbers is a little more complex. During the growing phase of the clouds, as in CAM, the precipitation rate decreases. But during the decaying phase, the precipitation rate actually increases even though the LWP decreases.

Figure 2a–c show the domain-averaged potential temperatures (θ), total water specific humidity (q_t), and cloud water content (q_c) at three different times (13:00, 14:00, and 15:00) from two CRM cases with surface aerosol numbers equal to 250 cm^{-3} (dash-dotted curves) and 1000 cm^{-3} (solid curves). q_t is the sum of q_c , rain and water vapor mixing ratios, which is an invariant within the PBL for stable non-precipitating well-mixed stratocumulus. θ and q_t from the two cases almost overlap except near the cloud top at 14:00 and 15:00. Figure 2a shows the growth of the PBL. At

13:00 the clouds do not completely reside within the PBL as the top of the PBL is at about 1.2 km which is lower than the cloud top height ($\sim 1.5 \text{ km}$) shown in Fig. 2c. Figure 2b shows that q_t in the top half of the cloud (from ~ 1.2 – 1.5 km) is larger than q_t in the bottom half of clouds (from ~ 1 – 1.2 km) and q_t below the clouds at 13:00. This suggests that the top half of the clouds are not fully coupled with the surface and the cloud water in the top half of the clouds is strongly affected by the horizontally advected positive moisture flux. At 14:00 and 15:00, the advected moisture flux becomes negative and the PBL is high enough that the clouds reside fully within the top of the PBL and possess the characteristics of well-mixed stratocumulus. The domain-averaged long-wave cooling rate at the cloud top height is about 2 K h^{-1} and is offset by a short-wave heating of about 0.5 K h^{-1} . Figure 2c shows that the cloud top is a little higher for the higher aerosol case, but the maximum values of q_c are smaller. A closer look at θ in Fig. 2a also shows that the top of the PBL which is near 1.5 km is higher and colder in the higher aerosol number case. These differences of q_c and

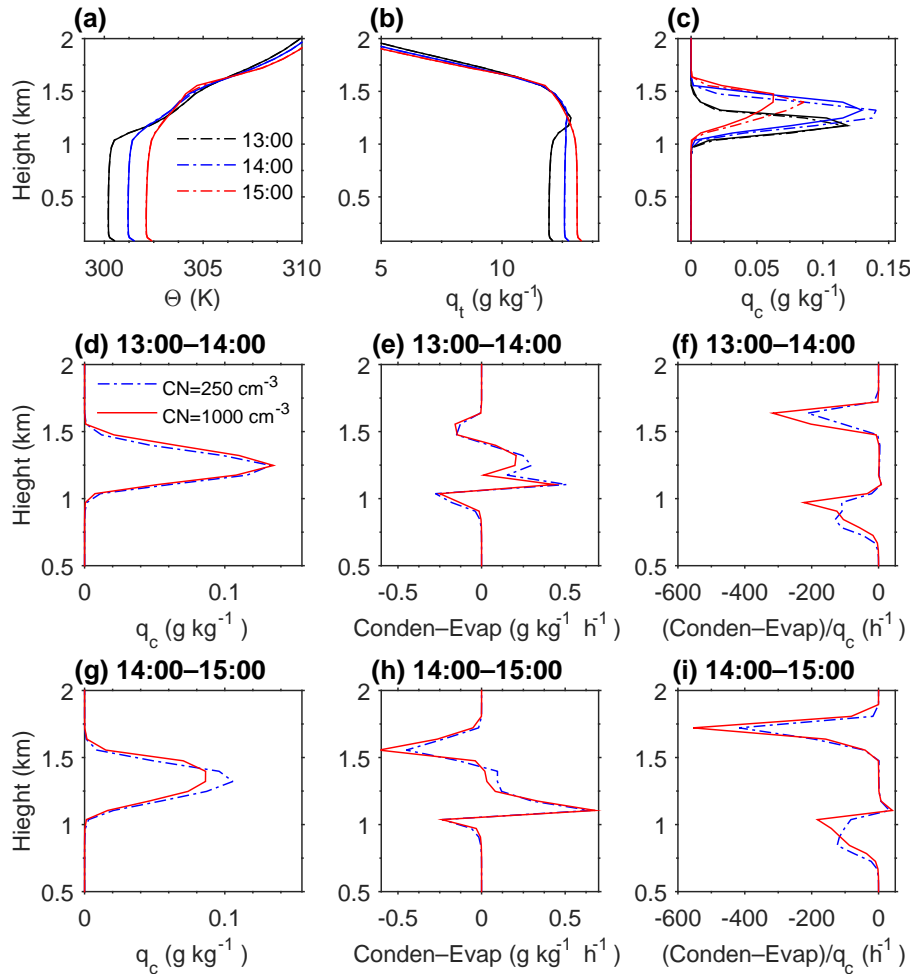


Figure 2. (a–c) Domain-averaged potential temperatures (θ), total water specific humidity (q_t), and cloud water content (q_c) at three different times (13:00, 14:00, and 15:00) from two GCE cases with surface aerosol numbers equal to 250 cm^{-3} (dash-dotted curves) and 1000 cm^{-3} (solid curves). (d–f) Averaged profiles of q_c , net results of condensation and evaporation (Conden–Evap), and (Conden–Evap)/ q_c for the 1 h interval from 13:00 to 14:00 from the two CRM cases with surface aerosol numbers equal to 250 cm^{-3} (blue dash-dotted curves) and 1000 cm^{-3} (solid red curves). (g–i) Same as (d–f) except for the 1 h interval from 14:00 to 15:00.

θ between the two cases are clearer in an enlarged portion of Fig. 2a and b shown in Fig. S3. The potential temperature in the sub-cloud layer at 14:00 and 15:00 is also slightly higher (about 0.005 K) for higher aerosols. Figure 2d–i show the time-averaged profiles of q_c and the net result of condensation and evaporation (Conden–Evap) during two 1 h intervals (Fig. 2d–f for 13:00 to 14:00 and Fig. 2g–i for 14:00 to 15:00) representing the growing and decaying phases of the cloud, respectively. Figure 2e and h show that a net evaporation occurs just below the cloud base and near the cloud top. The largest net condensation is located near the cloud base. The most obvious change between the growing phase and decaying phase of the cloud is the increased evaporation near the cloud top, especially for the high aerosol number case (see the changes from blue curve to the red curve at around 1.5 km from Fig. 2e and h). Choosing (Conden – Evap)/ q_c

as a measure of the inverse of the characteristic evaporation time of cloud droplets, Fig. 2f and i show that it increases substantially from 300 h^{-1} to about 600 h^{-1} (an evaporation time of $\sim 6 \text{ s}$) near the cloud top for the higher aerosol number case.

Figure 3 shows the LWP and the column-integrated LWP source and sink terms from the low and high aerosol cases (250 and 1000 cm^{-3}). The source term for LWP only includes the net condensation term (Conden – Evap) while the loss terms include autoconversion and accretion. Since CAM includes a separate autoconversion and accretion terms while GCE does not, we combined autoconversion and accretion as one term (Auto + Accre) for easier comparison. As shown in Fig. 1, when we increase the aerosol numbers from 250 to 1000 cm^{-3} , the LWP increase is relatively small in GCE and substantially larger in CAM. Both models show de-

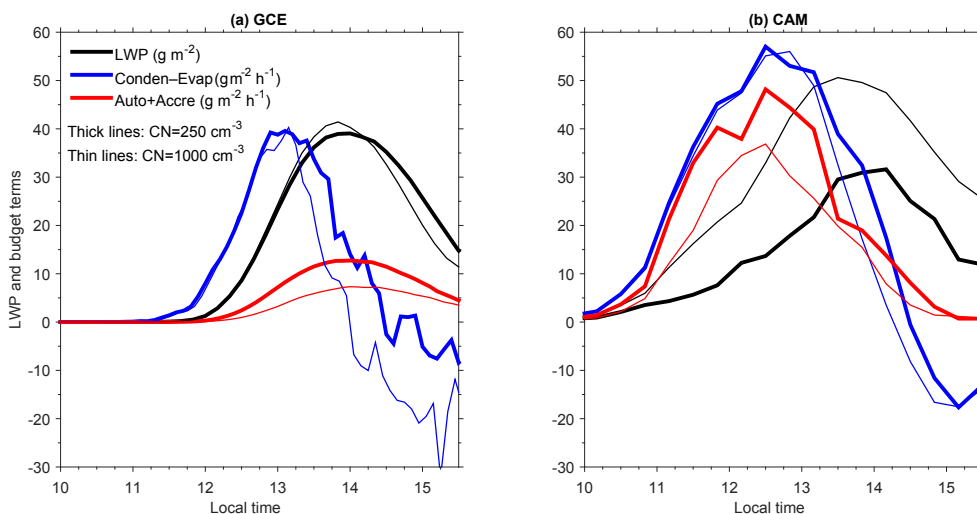


Figure 3. LWP and the column-integrated LWP source and sink terms from the cases with surface aerosol number concentration equal to 250 cm^{-3} (thick lines) and 1000 cm^{-3} (thin lines) for (a) GCE and (b) CAM.

creased Auto + Accre which acts to increase the LWP. This is expected as increased aerosol numbers increase the cloud droplet number which decreases the autoconversion rate. But CAM shows much larger changes, especially before 13:00. This is due to the fact that the two models use different cloud droplet activation schemes as well as schemes to parameterize the autoconversion and accretion processes. Since the autoconversion rate is directly affected by the aerosol number, we used an offline model to compare the autoconversion rates from the GCE and those from the Khairoutdinov and Kogan (2000) scheme used in CAM. The results are shown in Fig. S4. Compared to CAM's scheme, autoconversion rates from the GCE are less sensitive to the droplet number concentrations when the number concentrations are less than 100 cm^{-3} and the cloud mass mixing ratio is above 0.1 g kg^{-1} . When the cloud number concentrations are larger than 200 cm^{-3} , the autoconversion rates from GCE have a larger dependence on the number concentrations than those from the CAM scheme. However, they have a larger dependence on cloud mass mixing ratio than those from the CAM. So increasing aerosol number tends to decrease the autoconversion rate more in CAM than in GCE. As an example, we extracted the two pairs of in-cloud droplet number concentrations and mass mixing ratios ($[26\text{ cm}^{-3}, 0.167\text{ g kg}^{-1}]$) and ($[122\text{ cm}^{-3}, 0.293\text{ g kg}^{-1}]$) from the center layer of clouds at 11:30 from the two CAM cases in which the surface aerosol number increased from 250 to 1000 cm^{-3} . When applying CAM's scheme to these two pairs of data, the autoconversion rate decreases from 1.86×10^{-9} to $4.67 \times 10^{-10}\text{ kg kg}^{-1}\text{ s}^{-1}$. In GCE's scheme, the autoconversion rate only decreases from 1.57×10^{-9} to $1.48 \times 10^{-9}\text{ kg kg}^{-1}\text{ s}^{-1}$. Moreover, in GCE, the decreased autoconversion is largely offset or even outweighed by increased evaporation. As shown in Fig. 2e and h the increased evaporation occurs near the cloud top.

The increased evaporation near the cloud top and the higher PBL suggests that higher aerosol number concentrations lead to smaller cloud droplet sizes and enhanced evaporation at the cloud top which can then decrease the temperature slope near the cloud top and promote the sinking of entrained air into the cloud layer, a point made previously by Bretherton et al. (2007). This evaporation–entrainment feedback mechanism was also observed in small cumulus clouds (Small et al., 2009). Before $\sim 14:00$, the effect from the decreased autoconversion rates outweighs the effect from increased evaporation so that the LWP shows a slight increase. But as the cloud starts to decay after $\sim 14:00$, the PBL keeps growing and the enhanced evaporation/entrainment rates accelerate the decaying process. Thus, the LWP decreases faster and eventually a smaller LWP results over the decaying period for the high aerosol case. In the CAM, the change of the net condensation term (Conden – Evap) is smaller than that in the CRM. Since the simulated cloud top remains unchanged between 12:00 and 15:00, the drying effect seen in the CRM due to enhanced entrainment of overlying dry air is not present. This is likely due to the fact that the moist turbulence scheme in CAM does not depend on the cloud droplet number/size and the condensation and evaporation in the CAM's microphysics scheme is not linked to the cloud droplet number or size. Even though the instantaneous evaporation of falling cloud droplets into the clear portions of grids beneath clouds in the microphysics scheme is related to the cloud droplet number, it is about 1 order of magnitude smaller than the net condensation term in the macrophysics scheme. Consequently the net condensation and evaporation is less sensitive to the change in aerosol number and the effect from the decreased autoconversion rate dominates the condensate loss, leading to an increase of the LWP.

To confirm that the effect from enhanced entrainment at the cloud top is the critical reason for the reduced LWP change in GCE, we ran a sensitivity test to reduce the cloud top mixing by increasing the horizontal grid spacing from 50 m to 100 km. With this larger grid spacing, we greatly reduced the overshooting at the cloud top by reducing the maximum vertical speed in the updrafts from meters per second to a few centimeters per second. As a result, the enhanced entrainment effect was reduced and the microphysical effect from the reduced autoconversion rate dominated. Figure 4 shows that the LWP from GCE decreases by about 5 % for the $dx = 50$ m case while it increases by about 12 % for the $dx = 100$ km case when the surface aerosol number is increased from 250 to 4000 cm^{-3} . We also ran two more tests to explore whether the LWP sensitivity in CAM could match that in the GCE. In the default setup of CAM, the autoconversion rate is inversely proportional to cloud droplet number ($\sim N_c^{-1.79}$ where N_c is the in-cloud cloud droplet number). We ran two cases, auto06 and auto00, each with a reduced dependence of the autoconversion rate on the cloud droplet number. In the case auto06, the autoconversion rate is proportional to $N_c^{-0.60}$ and in the case auto00, the autoconversion rate does not depend on the cloud droplet number. The autoconversion rate is scaled in both cases to produce the same rate as that from the default case at a droplet number concentration of 100 cm^{-3} . As shown in Fig. 4, the LWP from the default case is more than doubled when the surface aerosol number is increased from 250 to 4000 cm^{-3} while the LWP from auto06 only increases by $\sim 50\%$ and the LWP from case auto00 remains almost unchanged. These results suggest that the dependence of the autoconversion rate on the cloud droplet number can play a determining role on the simulated LWP consistent with the findings of precipitation frequency susceptibility in Wang et al. (2012). However, this adjustment is unable to simulate decreases in LWP seen in the GCE model.

4 Conclusion and discussion

We simulated shallow warm clouds on 27 May 2011 at the DOE ARM SGP site with a cloud resolving model (Godard Cumulus Ensemble model) and a single-column model (CAM) using the same initial/boundary conditions and advected moisture/heat tendencies derived from the MC3E campaign data. The liquid water path (LWP) simulated by CAM shows a large dependence on the aerosol loading and is more than doubled when the surface aerosol number is increased from 250 to 4000 cm^{-3} while the LWP simulated by the CRM decreases by $\sim 5\%$. The high sensitivity of LWP on aerosol loading in CAM can be reduced by reducing the dependence of the autoconversion rate on the cloud droplet number concentration, but is unable to reproduce the decrease in LWP seen in the CRM. While Wang et al. (2012) concluded that this term in GCMs can be tuned to fit ob-

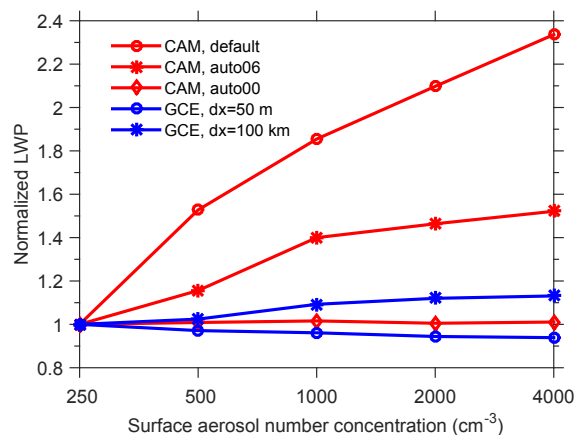


Figure 4. Normalized LWP as a function of surface aerosol concentration from CAM (red curves) and GCE (blue curves). A case for CAM using an autoconversion rate proportional to $N_d^{-0.6}$ (CAM, auto06) as well as a case in which autoconversion is independent of N_d (CAM, auto00) is shown. The GCE model was run with a horizontal grid resolution of 50 m (default case) and 100 km.

servations of the precipitation frequency susceptibility, we find that the poor representation of entrainment and droplet evaporation in CAM may be the fundamental cause of differences with the more complete CRM. While in the CRM a reduced autoconversion rate is also observed with increased aerosol loading, it is offset or even outweighed by the increased evaporation of cloud droplets near the cloud top. The increased evaporation cools the cloud top, reduces the temperature lapse rate and thus increases the entrainment of drier air above the cloud top and accelerates the decaying process of the clouds. Reduced LWP through enhanced entrainment with increased aerosol number has also been reported in previous literature using large eddy simulations (e.g., Ackerman et al., 2004; Bretherton et al., 2007; Seifert et al., 2015). To some extent our case is similar to the DYCOMS-II case studied in Ackerman et al. (2004) with low humidity above the cloud top. Our case has even less drizzle and this makes the increased entrainment effect even more dominant than the decreased drizzling effect, which explains why we only see decreased LWP with increasing aerosol concentrations.

One unique aspect of the present paper is that the response of the LWP over the lifetime of the cloud is negative in the CRM while it is positive in the CAM for the same forcing conditions. One critical deficiency of CAM for this case is that the effect from increased mixing of drier air from above the cloud layer through enhanced entrainment caused by increased aerosol numbers is missing. First, CAM is not able to simulate the growth of the cloud top due to its coarse vertical resolution. However, even if the CAM vertical resolution were high enough to capture the growth of the cloud top, since the moist turbulence scheme and the evaporation of cloud condensate in the cloud macrophysics parameteriza-

tion at the cloud top are not related to the cloud droplet number, aerosol number will not have a direct impact on the cloud top mixing or the LWP. Some effort has been made to address this issue in CAM. Jones (2013) implemented a droplet sedimentation–entrainment feedback scheme in CAM. Yet a mixture of the cloud macrophysics and the MG microphysics still prevent clouds from responding to droplet number changes by thinning or thickening as demonstrated by other LESs.

Our CRM results also demonstrate that the relative importance of the decreased autoconversion rate effect and the enhanced entrainment effect from increased aerosol numbers can change based on environmental conditions as manifested in different stages during the cloud life cycle. Thus, one may need to distinguish the cloud stage when studying the aerosol lifetime effect either with a model or from observations.

5 Data availability

Model outputs to generate all figures are available upon request. Source codes and model setups needed to repeat all CAM simulations are also available upon request.

The Supplement related to this article is available online at doi:10.5194/acp-17-21-2017-supplement.

Acknowledgements. This work was supported by the DOE under the grant number DOE DE-SC0008486. We thank Derek Posselt and S.-S. Lee for helpful discussions and setting up the GCE model, Shaocheng Xie for providing the ARM forcing data, and two reviewers (Steven Ghan and another anonymous reviewer) who greatly helped improve this work. We acknowledge high-performance computing support from National Energy Research Scientific Computing Center (NERSC).

Edited by: B. Ervens

Reviewed by: S. J. Ghan and one anonymous referee

References

Abdul-Razzak, H. and Ghan, S.: A parameterisation of aerosol activation 2. Multiple aerosol types, *J. Geophys. Res.*, 105, 6837–6844, 2000.

Ackerman, A. S., Kirkpatrick, M. P., Stevens, D. E., and Toon, O. B.: The impact of humidity above stratiform clouds on indirect aerosol climate forcing, *Nature*, 432, 1014–1017, 2004.

Albrecht, B. A.: Aerosols, cloud microphysics, and fractional cloudiness, *Science*, 245, 1227–1230, 1989.

Boucher, O., Randall, D., Artaxo, P., Bretherton, C., Feingold, G., Forster, P., Kerminen, V.-M., Kondo, Y., Liao, H., Lohmann, U., Rasch, P., Satheesh, S. K., Sherwood, S., Stevens, B., and Zhang,

X. Y.: Clouds and aerosols, in *Climate Change 2013: The Physical Science Basis*, Contribution of Working Group I to the Fifth Assessment Report of the Intergovernmental Panel on Climate Change, edited by: Stocker, T. F., Qin, D., Plattner, G.-K., Tignor, M., Allen, S. K., Boschung, J., Nauels, A., Xia, Y., Bex, V., and Midgley, P. M., Cambridge Univ. Press, Cambridge, UK, 2013.

Bretherton, C. S., Blossey, P. N., and Uchida, J.: Cloud droplet sedimentation, entrainment efficiency, and subtropical stratocumulus albedo, *Geophys. Res. Lett.*, 34, L03813, doi:10.1029/2006GL027648, 2007.

Chen, Y.-C., Christensen, M. W., Xue, L., Sorooshian, A., Stephens, G. L., Rasmussen, R. M., and Seinfeld, J. H.: Occurrence of lower cloud albedo in ship tracks, *Atmos. Chem. Phys.*, 12, 8223–8235, doi:10.5194/acp-12-8223-2012, 2012.

Chen, Y.-C., Christensen, M. W., Diner, D. J., and Garay, M. J.: Aerosol-cloudinteractions in ship tracks using TerraMODIS/MISR, *J. Geophys. Res.-Atmos.*, 120, 2819–2833, doi:10.1002/2014JD022736, 2015.

Christensen, M. W. and Stephens, G. L.: Microphysical and macrophysical responses of marine stratocumuluspolluted by underlying ships: Evidence of cloud deepening, *J. Geophys. Res.*, 116, D03201, doi:10.1029/2010JD014638, 2011.

Ghan, S., Randall, D., Xu, K.-M., Cederwall, R., Cripe, D., Hack, J., Iacobellis, S., Klein, S., Krueger, S., Lohmann, U., Pedretti, J., Robock, A., Rotstain, L., Somerville, R., Stenchikov, G., Sud, Y., Walker, G., Xie, S., Yio, J., and Zhang, M.: A comparison of single column model simulations of summertime midlatitude continental convection, *J. Geophys. Res.*, 105, 2091–2124, 2000.

Jones, C.: Single-column and mixed-layer model analysis of subtropical stratocumulus response mechanisms relevant to climate change, PhD thesis, University of Washington, 2013.

Khairoutdinov, M. F. and Kogan, Y.: A new cloud physics parameterization in a large-eddy simulation model of marine stratocumulus, *Mon. Weather Rev.*, 128, 229–243, 2000.

Klemp, J. B. and Wilhelmson, R. B.: The simulation of three-dimensional convective storm dynamics, *J. Atmos. Sci.*, 35, 1070–1096, 1978.

Lee, S. S. and Penner, J. E.: Comparison of a global-climate model to a cloud-system resolving model for the long-term response of thin stratocumulus clouds to preindustrial and present-day aerosol conditions, *Atmos. Chem. Phys.*, 10, 6371–6389, doi:10.5194/acp-10-6371-2010, 2010.

Lee, S. S., Penner, J. E., and Saleeby, S. M.: Aerosol effects on liquid-water path of thin stratocumulus clouds, *J. Geophys. Res.*, 114, D07204, doi:10.1029/2008JD010513, 2009.

Moncrieff, M. W., Krueger, S. K., Gregory, D., Redelsperger, J.-L., and Tao, W.-K.: GEWEX Cloud System Study (GCSS) Working Group 4: Precipitating convective systems, *B. Am. Meteorol. Soc.*, 78, 831–845, 1997.

Morrison, H. and Gettelman, A.: A new two-moment bulk stratiform cloud microphysics scheme in the NCAR Community Atmosphere Model (CAM3), Part I: Description and numerical tests, *J. Climate*, 21, 3642–3659, 2008.

Morrison, H., Curry, J. A., and Khvorostyanov, V. I.: A new double-moment microphysics parameterization for application in cloud and climate models. part i: Description, *J. Atmos. Sci.*, 62, 1665–1677, 2005.

- Neale, R. B., Gettelman, A., Park, S., Conley, A. J., Kinnison, D., Marsh, D., Smith, A. K., Vitt, F., Morrison, H., Cameron-Smith, P., Collins, W. D., Iacono, M. J., Easter, R. C., Liu, X., and Taylor, M. A.: Description of the NCAR Community Atmosphere Model (CAM 5.0), NCAR Tech. Note NCAR/TN-485CSTR, Natl. Cent. for Atmos. Res., Boulder, Co, 289 pp., 2012.
- Saleeby, S. M. and Cotton, W. R.: A large droplet mode and prognostic number concentration of cloud droplets in the Colorado State University Regional Atmospheric Modeling System (RAMS). Part I: Module descriptions and supercell test simulations, *J. Appl. Meteor.*, 43, 182–195, 2004.
- Seifert, A., Heus, T., Pincus, R., and Stevens, B.: Large-eddy simulation of the transient and near-equilibrium behavior of precipitating shallow convection, *J. Adv. Model. Earth Syst.*, 7, 1918–1937, doi:10.1002/2015MS000489, 2015.
- Small, J. D., Chuang, P. Y., Feingold, G., and Jiang, H.: Can aerosol decrease cloud lifetime?, *Geophys. Res. Lett.*, 36, L16806, doi:10.1029/2009GL038888, 2009.
- Smith, R. N. B.: A scheme for predicting layer clouds and their water content in a general circulation model, *Q. J. Roy. Meteor. Soc.*, 116, 435–460, 1990.
- Smolarkiewicz, P. K. and Grabowski, W. W.: The multidimensional positive advection transport algorithm: Nonoscillatory option, *J. Comput. Phys.*, 86, 355–375, 1990.
- Soong, S.-T. and Ogura, Y.: Response of tradewind cumuli to large-scale processes, *J. Atmos. Sci.*, 37, 2035–2050, 1980.
- Tao, W.-K. and Simpson, J.: The Goddard Cumulus Ensemble Model. Part I: model description, *Terr. Atmos. Ocean. Sci.*, 4, 35–72, 1993.
- Tao, W. K., Simpson, J., Baker, D., Braun, S., Chou, M. D., Ferrer, B., Johnson, D., Khain, A., Lang, S., Lynn, B., Shie, C. L., Starr, D., Sui, C. H., Wang, Y., and Wetzell, P.: Microphysics, radiation and surface processes in the Goddard Cumulus Ensemble (GCE) model, *Meteorol. Atmos. Phys.*, 82, 97–137, doi:10.1007/S00703-001-0594-7, 2003.
- Tao, W., Chen, J., Li, Z., Wang, C., and Zhang, C.: Impact of aerosols on convective clouds and precipitation, *Rev. Geophys.*, 50, RG2001, doi:10.1029/2011RG000369, 2012.
- Tao, W. K., Lang, S., Zeng, X. P., Li, X. W., Matsui, T., Mohr, K., Posselt, D., Chern, J., Peters-Lidard, C., Norris, P. M., Kang, I. S., Choi, I., Hou, A., Lau, K.-M., and Yang, Y.-M.: The Goddard Cumulus Ensemble model (GCE): Improvements and applications for studying precipitation processes, *Atmos. Res.*, 143, 392–424, 2014.
- Wang, M., Ghan, S., Liu, X., L'Ecuyer, T. S., Zhang, K., Morrison, H., Ovchinnikov, M., Easter, R., Marchand, R., Chand, D., Qian, Y., and Penner, J. E.: Constraining cloud lifetime effects of aerosols using A-Train satellite observations, *Geophys. Res. Lett.*, 39, L15709, doi:10.1029/2012GL052204, 2012.
- Xie, S., Xu, K.-M., Cederwall, R. T., Bechtold, P., Genio, A. D. D., Klein, S. A., Cripe, D. G., Ghan, S. J., Gregory, D., Iacobellis, S. F., Krueger, S. K., Lohmann, U., Petch, J. C., Randall, D. A., Rotstayn, L. D., Somerville, R. C. J., Sud, Y. C., von Salzen, K., Walker, G. K., Wolf, A., Yio, J. J., Zhang, G. J., and Zhang, M.: Intercomparison and evaluation of cumulus parametrizations under summertime midlatitude continental conditions, *Q. J. Roy. Meteor. Soc.*, 128, 1095–1135, 2002.
- Xie, S., Zhang, M., Branson, M., Cederwall, R. T., Del Genio, A. D., Eitzen, Z. A., Ghan, S. J., Iacobellis, S. F., Johnson, K. L., Khairoutdinov, M., Klein, S. A., Krueger, S. K., Lin, W., Lohmann, U., Miller, M. A., Randall, D. A., Somerville, R. C. J., Sud, Y. C., Walker, G. K., Wolf, A., Wu, X., Xu, K.-M., Yio, J. J., Zhang, G., and Zhang, J.: Simulations of midlatitude frontal clouds by single-column and cloud-resolving models during the Atmospheric Radiation Measurement March 2000 cloud intensive operational period, *J. Geophys. Res.*, 110, D15S03, doi:10.1029/2004JD005119, 2005.
- Xie, S., Zhang, Y., Giangrande, S. E., Jensen, M. P., McCoy, R., and Zhang, M.: Interactions between cumulus convection and its environment as revealed by the MC3E sounding array, *J. Geophys. Res.-Atmos.*, 119, 11784–11808, doi:10.1002/2014JD022011, 2014.
- Xu, K.-M., Cederwall, R. T., Donner, L. J., Grabowski, W. W., Guichard, F., Johnson, D. E., Khairoutdinov, M., Krueger, S. K., Petch, J. C., Randall, D. A., Seman, C. J., Tao, W.-K., Wang, D., Xie, S. C., Yio, J. J., and Zhang, M.-H.: An inter-comparison of cloud-resolving models with the Atmospheric Radiation Measurement summer 1997 IOP data, *Q. J. Roy. Meteor. Soc.*, 128, 593–624, 2002.
- Xue, H. and Feingold, G.: Large-eddy simulations of trade wind cumuli: Investigation of aerosol indirect effects, *J. Atmos. Sci.*, 63, 1605–1622, doi:10.1175/JAS3706.1, 2006.